# 3. HAZARDOUS LIQUID PIPELINES

## 3.1 Technical Background

It is widely recognized that liquid pipelines can develop cracks in service due to stress corrosion and mechanical damage (e.g., impact from third party excavation equipment such as backhoes) in combination with subsequent fatigue. Conventional leak-before-break methodology based on linear elastic fracture mechanics provides criteria for determining if a part-through-crack which becomes unstable and penetrates (or pops through) the wall is likely to continue to grow unstably giving rupture [5,12]. In pipelines, the walls are sufficiently thin (0.3"-0.4" generally) and if the fracture toughness of pipeline steel is sufficient in magnitude, a part-through-crack which popped through the wall would need to be ~5-10" long to be unstable and continue to grow [13,14].

Recent work by Eiber and Bubenik [12] illustrates the results of the application of leak-before [or without)-rupture to pipeline steel. They calculated the failure stress for part-through-wall cracks for various combinations of crack depth and crack length for X52 steel. For the same steel, they also determined the critical length of a through-wall crack that would be required for unstable crack growth at various hoop stress levels. Their results are presented in Figure 17, which also includes experimental results (R indicates rupture and L indicates leak).

If one considers X52 steel pipe, the hoop stress at the maximum operating pressure would be ~0.72x52,000=37.4 ksi. For a hoop stress of 37 ksi (72% SMYS), a 30" diameter pipe with a 0.375" wall thickness and a part-through crack which is 61% of the way through the wall would need to be ~14" long to pop through, giving leakage. As seen in Figure 17, a 14" through-wall crack (twc) would only require 24 ksi to run, which is less than the 37 ksi to give pop through. Thus, rupture would occur immediately. At an operating stress of 72% of SMYS which is 37 ksi for a X52 steel, part-through-wall cracks of a usual length (~6") must grow to 70% to 80% of the wall thickness before they become unstable and penetrate the wall, becoming a through-crack. Figure 17 indicates such a crack would be stable since a 6" flaw at 37 ksi lies below the "twc" curve for growth of a through crack, indicating leakage without rupture (i.e., no subsequent unstable growth of through crack). It should be emphasized that the position of the "twc" curve depends on the value assumed for K, the dynamic stress intensity factor, while the position of the four part-through crack curves depends on the value selected for $K_{Ic}$, the critical stress intensity for plane strain conditions. Some of the experimental data for rupture versus leakage (labeled R or L on the graph) in Figure 17 are not consistent with the predictions, with several examples of rupture indicated below the through-wall crack (twc) curve, which defines the requires hoop stress for a given flaw size for unstable growth of the axial through-wall crack.

It is clear from the forgoing discussion that when a part-through wall crack reaches a size at which it grows unstably, becoming a through-wall crack, rupture may occur immediately (i.e., the through crack continues to grow unstably in the axial direction). Unlike unstable crack growth in a gas pipeline, instability in a hazardous liquid pipeline will give a more modest rupture, limited by the much quicker loss of internal pressure in the pipe as the crack grows in length and opens, allowing product to pour out of the pipe. If rupture does not occur immediately, subsequent time-dependent crack growth can still occur due to fatigue or stress corrosion cracking, allowing the through crack to reach a sufficient length that it can again grow

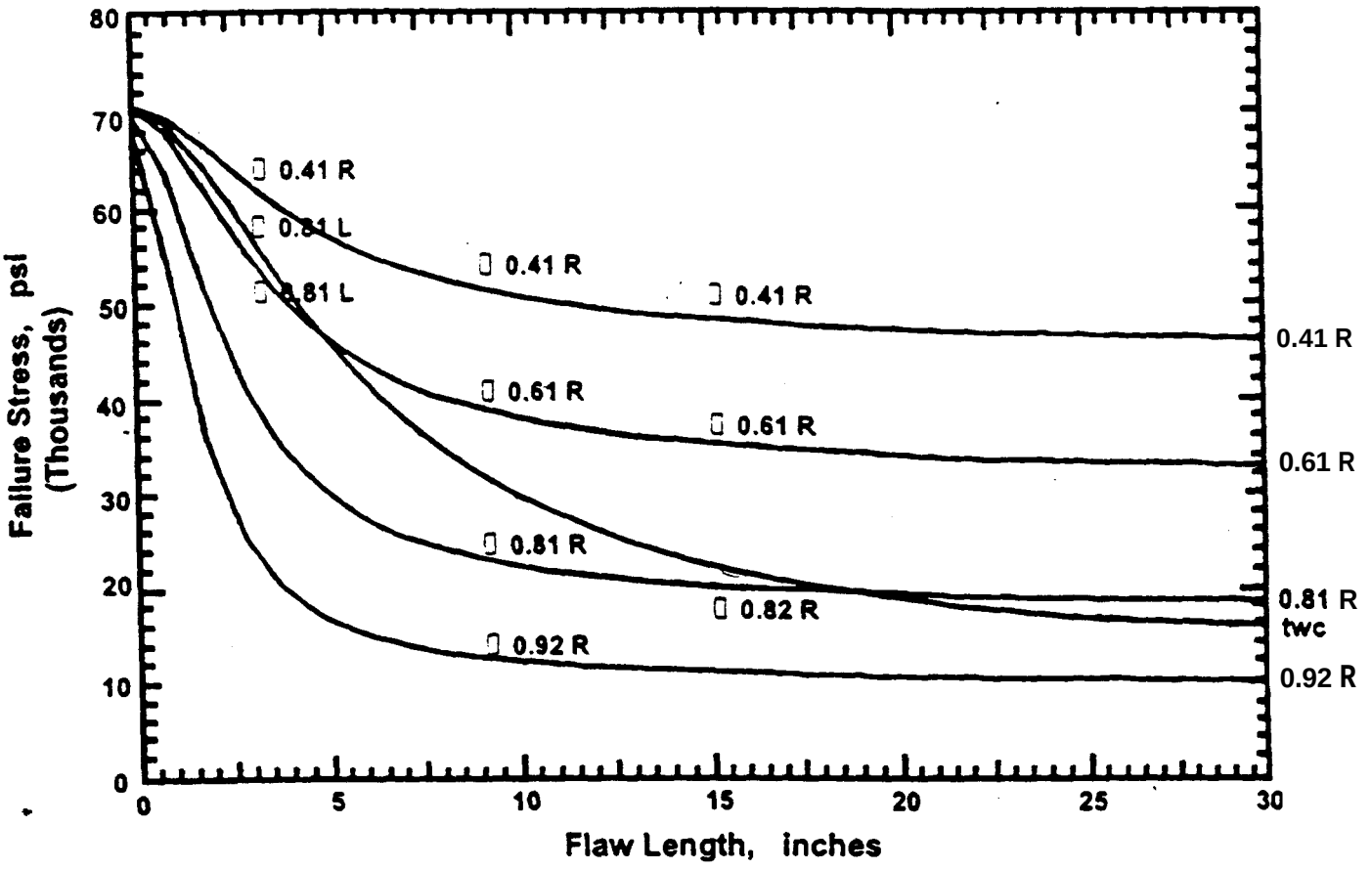


Figure 17 Critical flaw sues in 30-inch diameter by 0.375-inch thick (762by 9.5-mm) X52 (Grade 358) pipe compared to experimental data.

unstably, giving a significant rupture in the pipeline. Fatigue crack growth is more likely in liquid pipelines than in gas pipelines due to the greater pressure fluctuations that occur in liquids than in gases, since liquids have higher bulk moduli. The time period between initial leakage and the subsequent slow, stable crack growth to a size that gives unstable axial crack growth and rupture may provide a window of opportunity wherein the leakage of product allows detection of the through crack before a more catastrophic failure occurs.

The analysis of the hazardous liquid pipeline problem using a leak-without-rupture fracture mechanics approach will be divided into two scenarios. First, we will consider the case of leakage-without-rupture using a classical linear elastic fracture mechanics analysis, to determine if the newly formed through crack will have a sufficiently high stress intensity to drive the crack in the axial direction where material resistance is measured by the critical dynamic stress intensity $K_d$. In the second scenario, we will use a J-integral approach to determine the critical length for the onset of unstable crack growth of an axial through-crack. Leak-without-(immediate) rupture can still result in eventual rupture as a consequence of the stable growth of the through-wall crack under the influence of fatigue stressing or stress corrosion cracking: In this second scenario, the allowable operating pressure and associated hoop stress to avoid rupture in a hazardous liquid pipeline will depend on both the toughness of the steel and the sensitivity of detection of leakage from the pipeline.

### 3.2 Analysis of Leak-Without-Rupture for Hazardous Liquid Pipelines: Case I - Avoiding Immediate Rupture at First Formation of a Through-Wail Crack

For purposes of illustration, the analysis of Kanninen and Popelar [5] for leak-without-rupture has been followed. Assuming a part-through-wall crack, the linear-elastic fracture mechanics criteria for the propagation of this semi-elliptical surface flaw is given by:

$$K_I = 1.12\frac{P_o R}{t}\left[\frac{\pi a}{Q}\sec\left(\frac{\pi}{2}\frac{a}{h}\right)\right]^{1/2} = K_{Ic} \qquad (13)$$

where Q, which is a geometric correction that takes into account the shape of the semi-elliptical surface flaw and is given by $1+1.464\,(a/c)^{1.65}$, is assumed to be equal to 1.0 (which assumes $a/c \ll 1.0$). The secant term is a geometric correction for the case where the crack depth, a, is a significant fraction of the wall thickness of the pipe, which is almost always the case for pipeline failures. $P_o$, is the pressure at the time the part-through-wall crack begins to propagate, and R and t are the pipe radius and wall thickness respectively. $K_{Ic}$ is the critical stress intensity for plane strain fracture for quasi-static loading and can range in value from 30 ksi $(in)^{0.5}$ to 240 ksi $(in)^{0.5}$ depending on whether the service temperature is on the lower or upper shelf for the pipeline steel.

Once the part-through-wall crack propagates unstably, becoming a through-wall crack, the question of whether it will continue to propagate axially can also be addressed using linear-elastic fracture mechanics as follows:

$$K_1 = \frac{P_1 R}{t}\left[\pi c\left(1 + 1.61\frac{c^2}{Rt}\right)\right]^{1/2} = K_d \qquad (14)$$

where $P_1$ is the pressure after the crack has become a through-wall crack and would take account of the decompression in the pipe due to leakage of product out the through-wall crack. The term inside the parentheses is the Folias correction for bending moment that would be present for axial crack growth in a cylinder which would not be present for growth of a through crack in a wide plate. $K_d$ is the critical dynamic stress intensity for the pipe, measuring the resistance to growth by a running crack (as distinct from quasi-static initiation, $K_{1c}$). On the upper shelf, this value may exceed K,, by as much as 80% due to the higher flow stress and the lower degree of constraint for crack growth in a thin walled pipe. However, dynamic crack growth in lower yield strength steels shifts the ductile to brittle transition temperature (DBTT) by as much as 100C. This shift in the DBTT can put the unstable crack propagation on the lower shelf, giving $K_d$ a value of 30-40 ksi $(in)^{0.5}$. Thus, the ratio of $K_d / K_{1c}$ can then vary from as large as 2.0 on the upper shelf, to values as low as 0.2 in the DBTT region and a value of ~ 1.0 when both quasi-static and dynamic fracture are brittle, giving lower shelf behavior.

If Equations (13) and (14) are divided with the quotient algebrically simplified, the resultant equation is:

$$\left[1 + 1.61\frac{t}{R}\left(\frac{c}{t}\right)^2\right]\left(\frac{c}{t}\right) = 1.25\left(\frac{K_d}{K_{1c}}\right)^2\left(\frac{P_o}{P_1}\right)^2 \frac{a}{t}\sec\left(\frac{\pi}{2}\frac{a}{t}\right) \qquad (15)$$

This equation defines the conditions for which a part-through-wall crack will propagate and the through-wall cracks which result will continue to run unstably, giving leak-with-rupture. If one specifies $\left\{\frac{K_d}{K_{1c}}\ \frac{P_o}{P_1}\right\}^2$ for a given pipe (R and t specified), a graphical representation can be made of c/t versus a/t, with values which fall above this curve defining conditions for leak-with-rupture and values which fall below this curve defining conditions for leak-without-rupture. Figures 18-21 give c/t versus a/t for several different combinations of pipe radius and wall thickness and for a variety of values for $\left\{\frac{K_d}{K_{1c}}\ \frac{P_o}{P_1}\right\}^2$. If the relevant critical stress intensities can be determined experimentally, then one can predict whether a given crack (a,c) will give leak-without-break.

More exacting solutions for the stress intensity for a part-through crack and for a through crack are available [15] to give improved accuracy over Equations (13) and (14) used above. These equations are as follows:

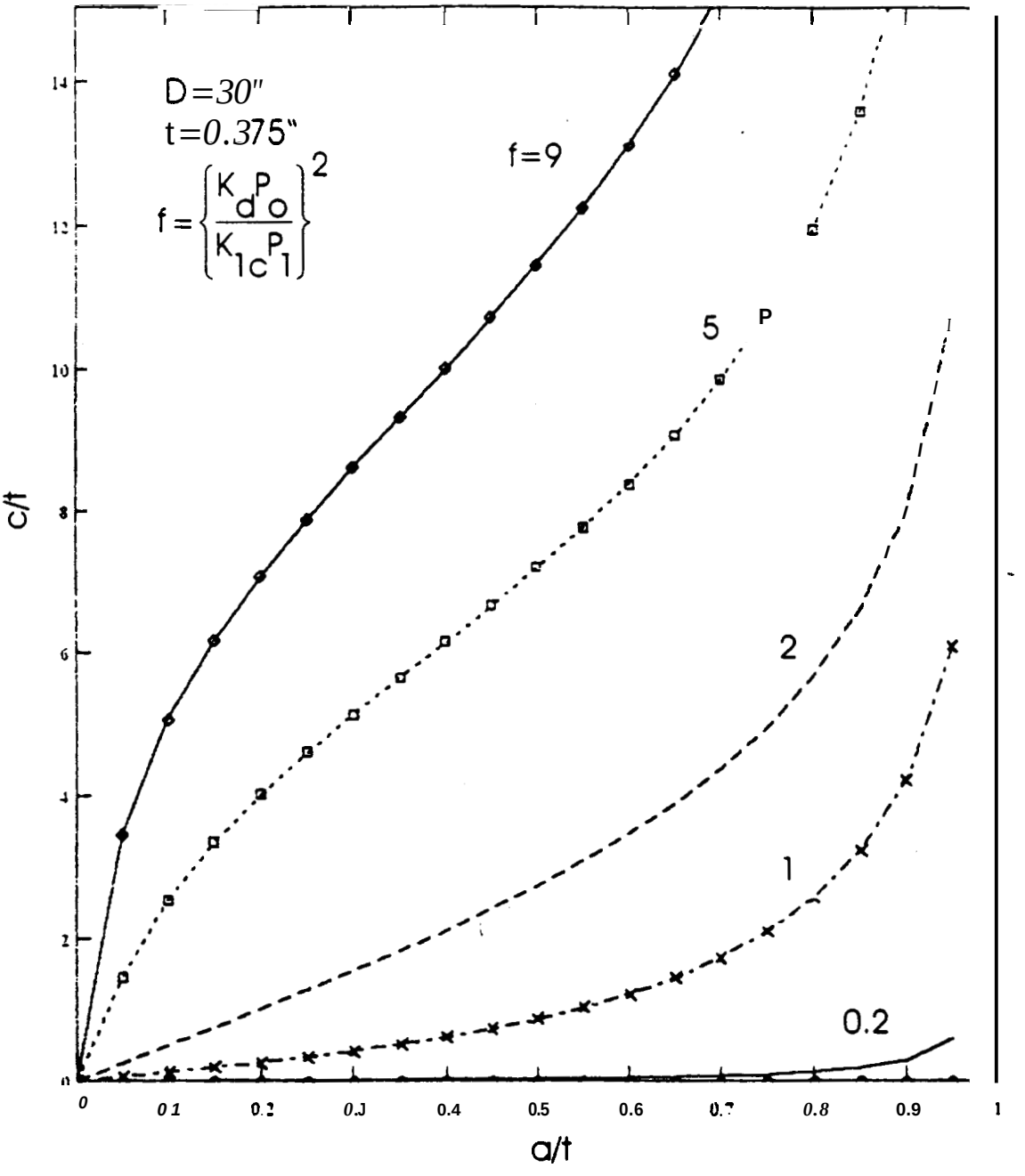


Figure 18 Results of leak-without-rupture analysis for various ratios of dynamic and quasi-static critical stress intensities and for ratios of initial pressure before leak $P_o$ and after leak but before rupture P, . If a given crack with an initial c/t and a/t value lies below the appropriate curve for a given "f" value, the leak-without-rupture occurs. Above the same curve corresponds to leak-with-rupture.

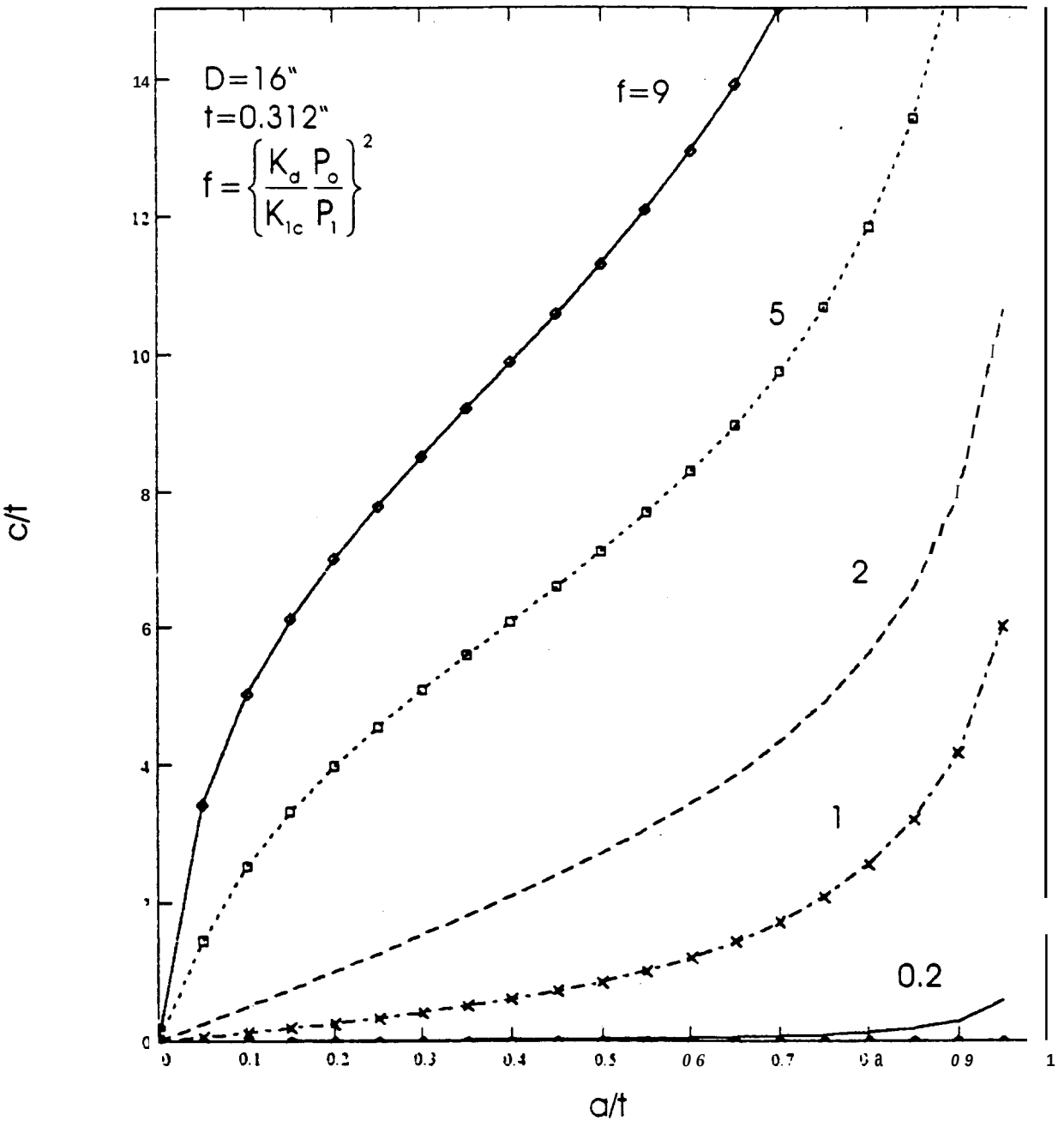


Figure 19 Results of leak-without-rupture analysis for various ratios of dynamic and quasi-static critical stress intensities and for ratios of initial pressure before leak $P_o$ and after leak but before rupture $P_1$. If a given crack with an initial c/t and a/t value lies below the appropriate curve for a given "f' value, the leak-without-rupture occurs. Above the same curve corresponds to leak-with-rupture.

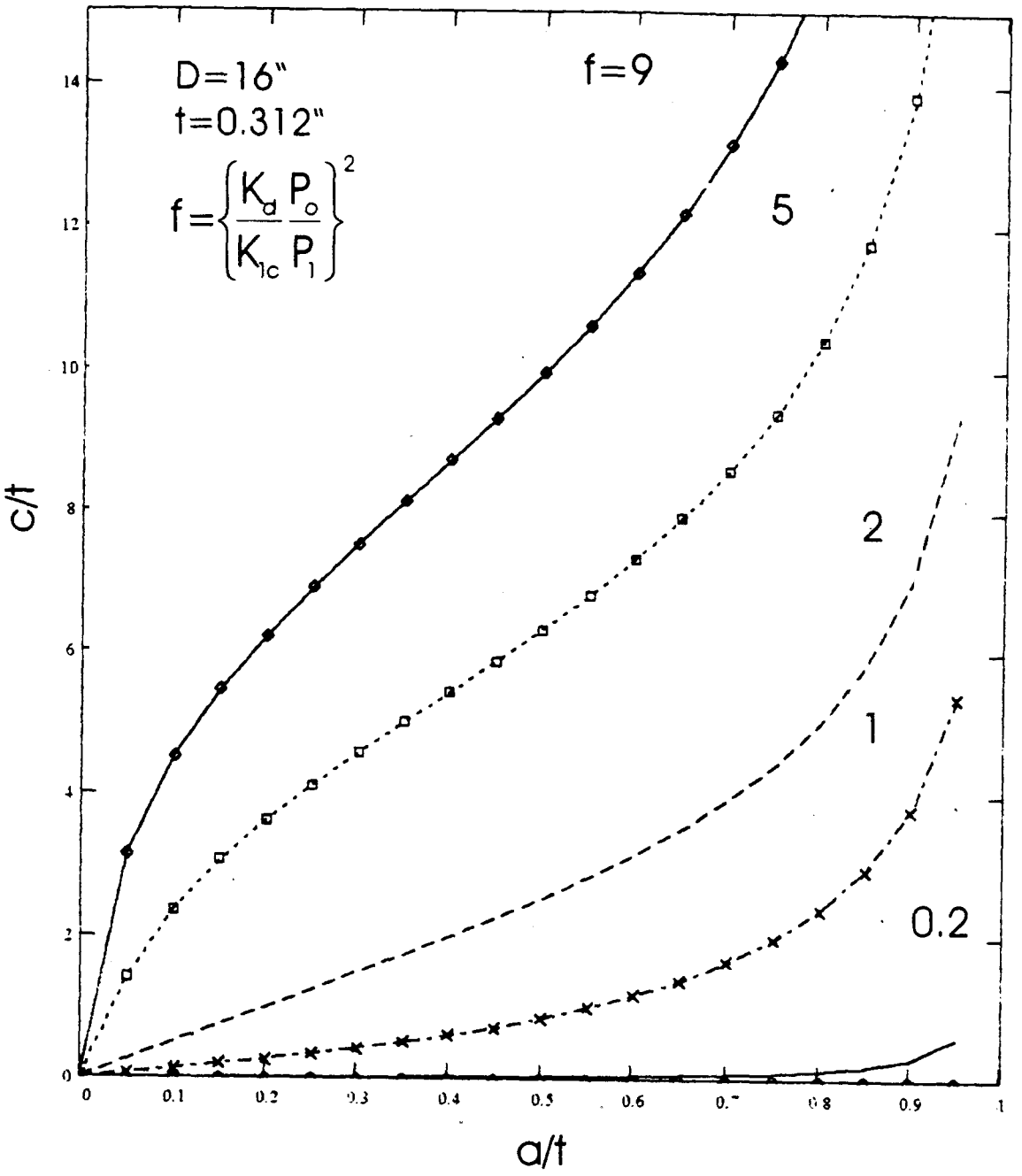


Figure **20** Results of leak-without-rupture analysis for various ratios of dynamic and quasi-static critical stress intensities and for ratios of initial pressure before leak $P_o$ and after leak **but** before rupture $P_1$. If a given crack with **an** initial c/t and a/t value lies below the appropriate curve for a given "f" value, the leak-without-rupture occurs. Above the same curve corresponds to leak-with-rupture.

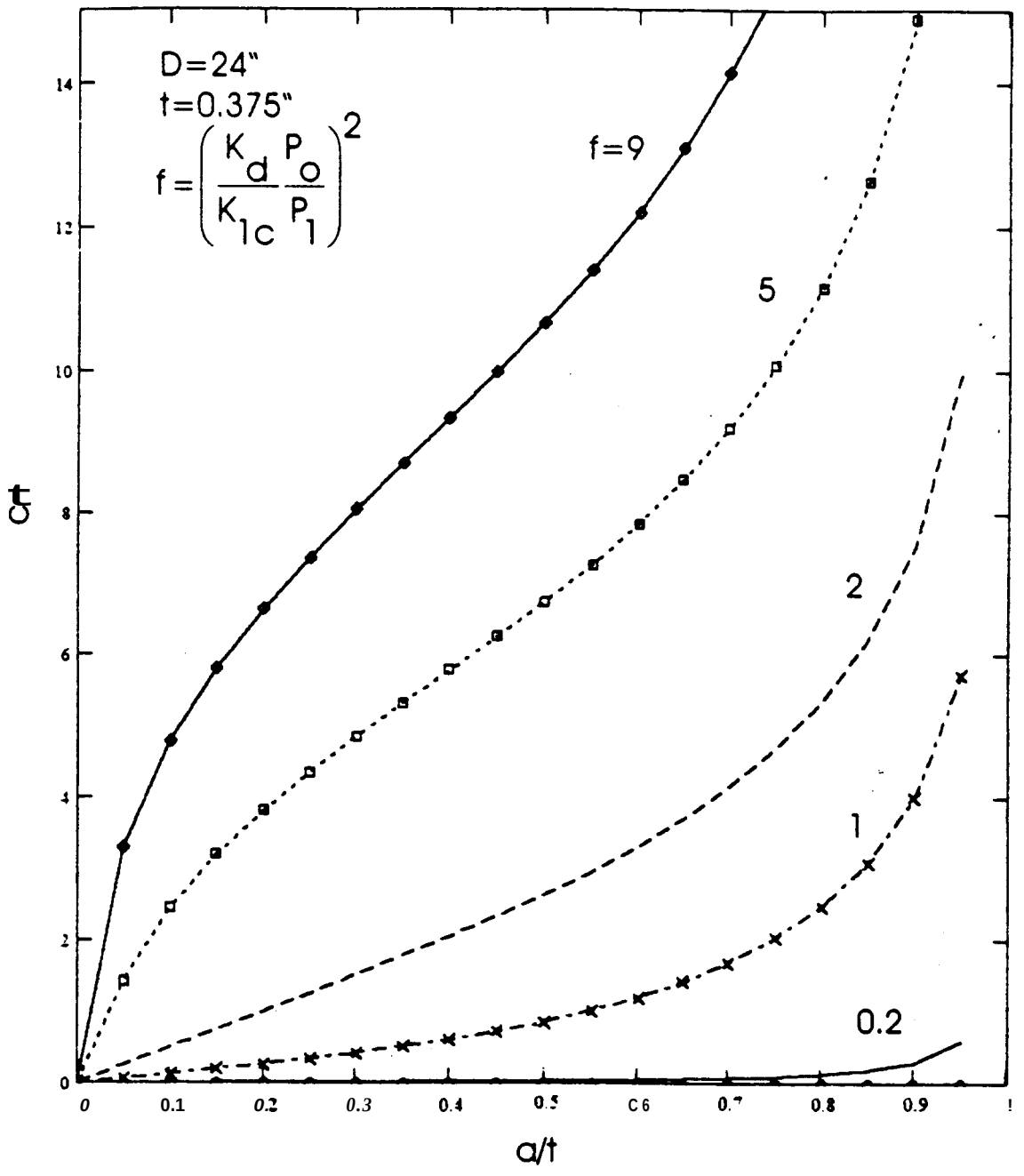


**Figure 21** **Results of leak-without-rupture analysis for various ratios of dynamic and quasi-static critical stress intensities and for ratios of initial pressure before leak $P_o$ and after leak but before rupture $P_1$. If a given crack with an initial c/t and a/t value lies below the appropriate curve for a given "f" value, the leak-without-rupture occurs. Above the same curve corresponds to leak-with-rupture.**

Part-through crack in a plate-

$$K_1 = f(\phi)\frac{P_o R}{t}\sqrt{\frac{\pi a}{Q}}\left[M_1 + M_2\left(\frac{a}{t}\right)^2 + M_3\left(\frac{a}{t}\right)^4\right] = K_{1c} \qquad (16)$$

where

$$Q = 1 + 1.464\left(\frac{a}{c}\right)^{1.65}$$

$$M_1 = 1.13 - 0.09\left(\frac{a}{c}\right)$$

$$M_2 = 0.89\left(0.2 + \frac{a}{c}\right)^{-1} - 0.54$$

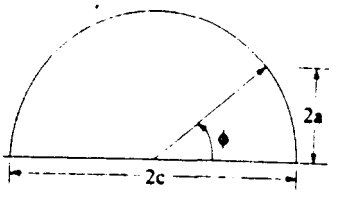


$$M_3 = 0.5 - \left[0.65 + \frac{a}{c}\right]^{-1} + 14\left[1.0 - \frac{a}{c}\right]^{24}$$

$$F(\phi) = \left[\frac{a^2}{c^2}\cos\phi + \sin^2\phi\right]^{1/4}$$

$$F(90^o) = 1 \qquad F(0^o) = \sqrt{\frac{a}{c}}$$

Axial through crack in a cylinder--

$$\frac{P_1 R}{t}\sqrt{\pi c}\left(1 + 0.52x + 1.29x^2 - 0.074^3\right) = k_d \qquad (17)$$

where $x = \dfrac{c}{\sqrt{Rt}}$

Using Equation (16), one may specify an initial crack depth a/t and then calculate the hoop stress ($P_o$ R/t) required to get the through crack to pop through as a function of the crack length 2c for a given value of $K_{1c}$. Using Equation 17, for a given value of $K_d$, the hoop stress as a function of crack length, 2c, can be calculated. Both results are presented in Figure 22. For a given a/t and flaw length, 2c, leak-without-rupture occurs if the hoop stress required for growth of the part-through crack lies below the stress required to propagate the through-wall crack. It is clear from Figure 22 that a $K_d$ of 40 ksi (in)$^{1/2}$ allows leak-with-rupture for almost any combination of a and c, except when the a/t at failure is 0.9, which is to say a very deep crack. On the other hand, when $K_{1c}$ is 120 ksi (in)$^{1/2}$, leak-without-rupture occurs for all cases except where the crack size is very shallow (i.e., a/t = 0.3), the crack length suitably long (i.e., 2c = >4"), and the hoop stress quite high (~100% SMYS).

Figures 18-21 clearly allow one to infer what is necessary to have leak-without-rupture; namely, a larger ratio of $K_d$ to $K_{1c}$ (corresponding to larger f values in the figures) or a large a/t

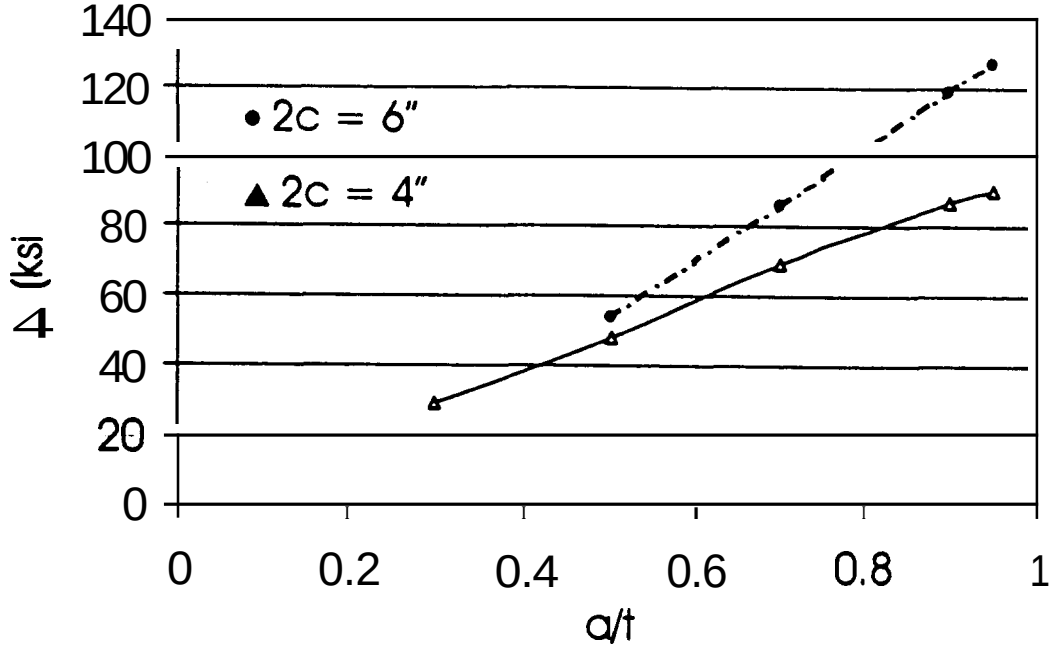


**Figure 22** Stress intensity as a function of a/t for a pipe with a part-through crack, with 2c= 4" or 6", for an internal pressure that is equivalent to 72% *SMYS*.

ratio corresponding to a larger K,,, as seen in Figure 22. The larger a/t ratio is easily seen in Equations (13) or (16) to increase with an increasing value of $(K_{Ic} \cdot t) / (P_o \cdot R)$, or the ratio of the critical stress intensity to the hoop stress. Thus, safe operation of hazardous liquid pipelines, by which we mean leak-without-rupture, is possible at the current operating stress level of 0.72SMYS if and only if the pipeline steel meets certain requirements for quasi-static and dynamic fracture toughness, as measured by the critical stress intensities for these two conditions. Such a conclusion is consistent with current understanding in industry [4], but defines the minimum required fracture toughness using critical stress intensities rather than Charpy V-notched tests or drop weight tear tests. For either approach, the operating temperature relative to the ductile to brittle transition temperature becomes a critical issue.

The ductile-brittle transition temperature is not an unique temperature is not an unique temperature for a given steel grade. There can be significant shift in the DBTT due to strain rate effects, chemical composition variations between line pipe lots and heats, and variation in the manufacturing processes. These variations are illustrated with the schematic shown in Figure 23 based on actual data from a variety of steels published in the literature. The shift in the transition temperature for fatigue precracked Charpy specimens compared to standard Charpy V-notched specimens is due to the smaller plastic zone and higher degree of constraint that occurs in crack initiation at a fatigue precrack compared to a relatively blunt V-notch. The shifts associated with the dynamic versus quasi-static behavior are the result of the rate dependence of the yield strength in low strength steels, with higher rates giving high yield strengths, small plastic zones at the crack or notch tip, and thus, a higher degree of constraint.

To apply the methodology developed in this section, one would need to experimentally reproduce the type of information illustrated in Figure 23 on a variety of X52 steels using 2/3rd size Charpy specimens cut from actual pipe. If the Charpy V-notched data can be used to determine the $K_{Ic}$ and $K_d$ values by a temperature shifting procedure or by direct correlations [16], then Charpy V-notched data which is readily available from the field could be used to assess the safety of liquid pipeline operations with regard to leak-without-rupture.

Case histories on file at the Office of Pipeline Safety in the Department of Transportation indicate that field ruptures are often associated with cracks which have an $a/t = 0.7\text{-}0.75$ with a length of approximately 5"-6" at the time that leak-with-rupture occurs [17]. Figs. 18-21 would predict for such pipelines with c/t values of approximately $2.5/0.312 = 8.0$, leak-with-rupture would occur except in the unlikely case of pipe with a $(K_d / K_{Ic})^2 = 4.0$, or the ratio of the two critical stress intensities equals 2.0, assuming no depressurization immediately after the crack penetrates the pipeline wall. It should be noted that crack propagation in liquid pipelines does eventually arrest after a short growth when the internal pressure P, drops sufficiently to increase "f' in Figures 18-21 to a value which is consistent with leak-without (further) rupture.

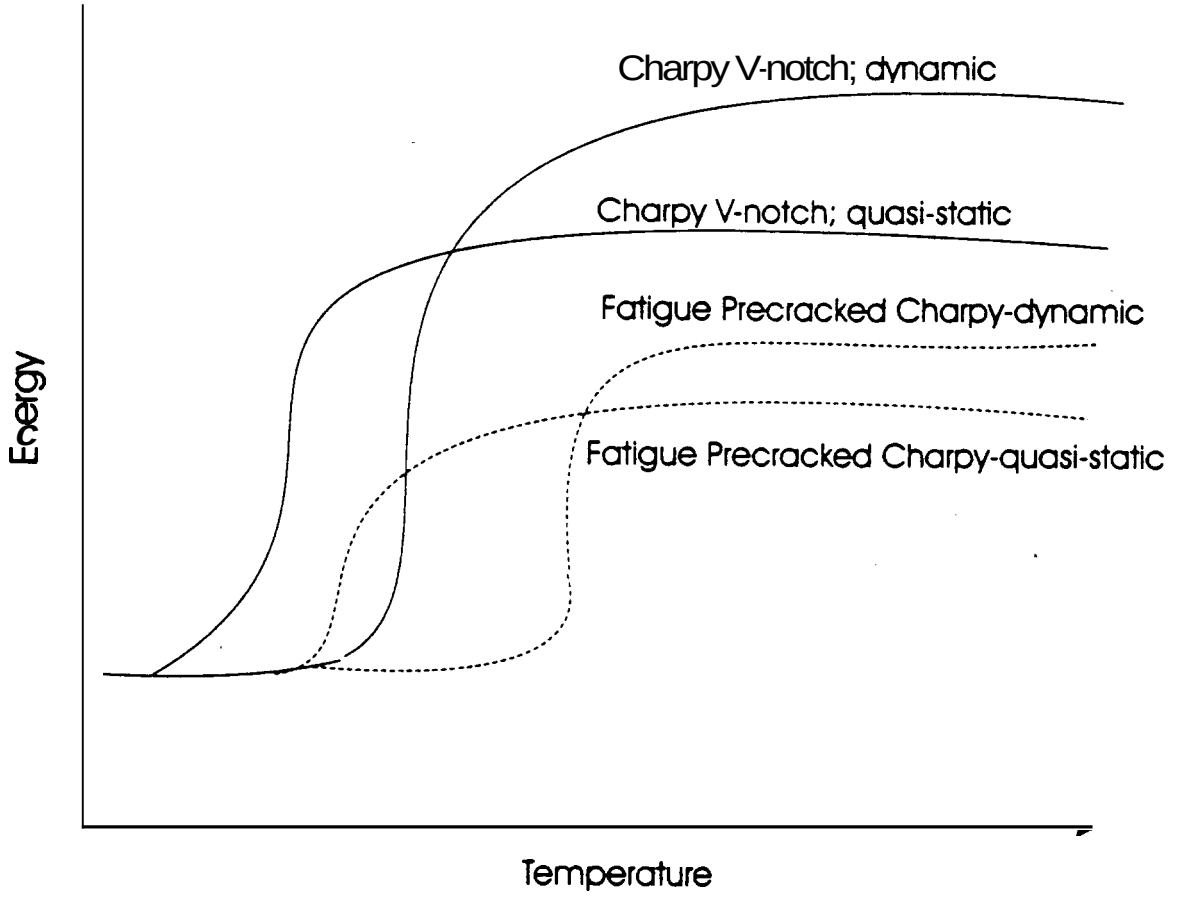


**Figure 23** **Schematic indicating the transition temperature as a function of loading rate (dynamic or static) and as a function of notch aquity (standard V-notch or fatigue precracked).**

A comparison of stress to form a through-wall crack ($K_{Ic}$ = 40 ksi $(in)^{0.5}$) to the stress required to propagate this through wall crack ($K_d$ ~ 40 or 120 ksi $(in)^{0.5}$) as a function of a/t and 2c is seen in Figure 24 for $\frac{P_0}{P_1}$ assumed to be equal to 1.0. For a given flaw length, 2c, if the stress to give pop-through (curves for various $K_{Ic}$ and a/t values) is greater than the stress required to propagate the crack (curves labled $K_d$), the leak-with-rupture will occur immediately. Note for (a/t)=0.7 and 2c=6 in, the stress to give a through crack ($K_{Ic}$ = 40 ksi $(in)^{0.5}$) is 20 ksi whereas that required to propagate this through crack ($K_d$=40 ksi $(in)^{0.5}$) is only 12 ksi $(in)^{0.5}$.

Finally, it should be mentioned that the analysis in this section has been conducted assuming failure by fracture phenomenon rather than by net section yielding and plastic collapse. Recent studies of fatigue crack growth in dented pipe at Texas A&M University indicates that fatigue cracks can grow all the way through the pipe wall without giving net section yielding and failure by plastic collapse. Such behavior would be predicted in thin walled pipe if $K_{Ic}$ > 200 ksi $(in)^{0.5}$. It is not clear whether a deeply penetrating crack results in load redistribution and/or local deformation which changes locally the radius of curvature to one that lowers the local stress sufficiently to avoid plastic collapse. In any case, an important assumption in this analysis is failure by crack growth rather than by plastic collapse.

In the next section, the scenario of a part-through crack going unstable and producing a stable through crack will be considered.

### 3.3 Analysis of Leak-Without Rupture for Hazardous Liquid Pipelines: Case 11--Time Dependent Stable Growth of a Through-Wall Crack Leading to Unstable Crack Growth and Rupture

In the previous section, the case of unstable growth of a part-through-wall crack, resulting in a through-wall crack which continues to grow unstably was considered. In this section, the alternative case of a part-through wall crack which grows unstably to form a stable through wall crack will be considered. In this case, this new through-wall crack can grow over time due to fatigue or stress corrosion cracking until it reaches a sufficient length to grow unstably, producing a sufficiently long crack to constitute rupture.

The analysis for leak-without-rupture for hazardous liquid pipelines involves four steps: (1) calculation of the J-integral as a function of the length of a through-crack, 2c, for hoop stresses corresponding to 40%, 50%, 60%, and 72% of the specified minimum yield strength, with these calculations being repeated for each of the four selected combinations of wall thickness and pipe diameters for both X52 and X60 steel; (2) comparison of J-c curves with J-A measurements taken on X52 and X60 steel to determine the crack length at instability, the amount of stable crack growth preceding instability, and the initial crack length, $2c_o$ - see Figure 18; (3) calculation of the area of opening which would result for each crack from (2) when the pipe is pressurized; and finally (4) calculation of the rate of leakage which would result from a pipe which has reached the critical size for rupture.

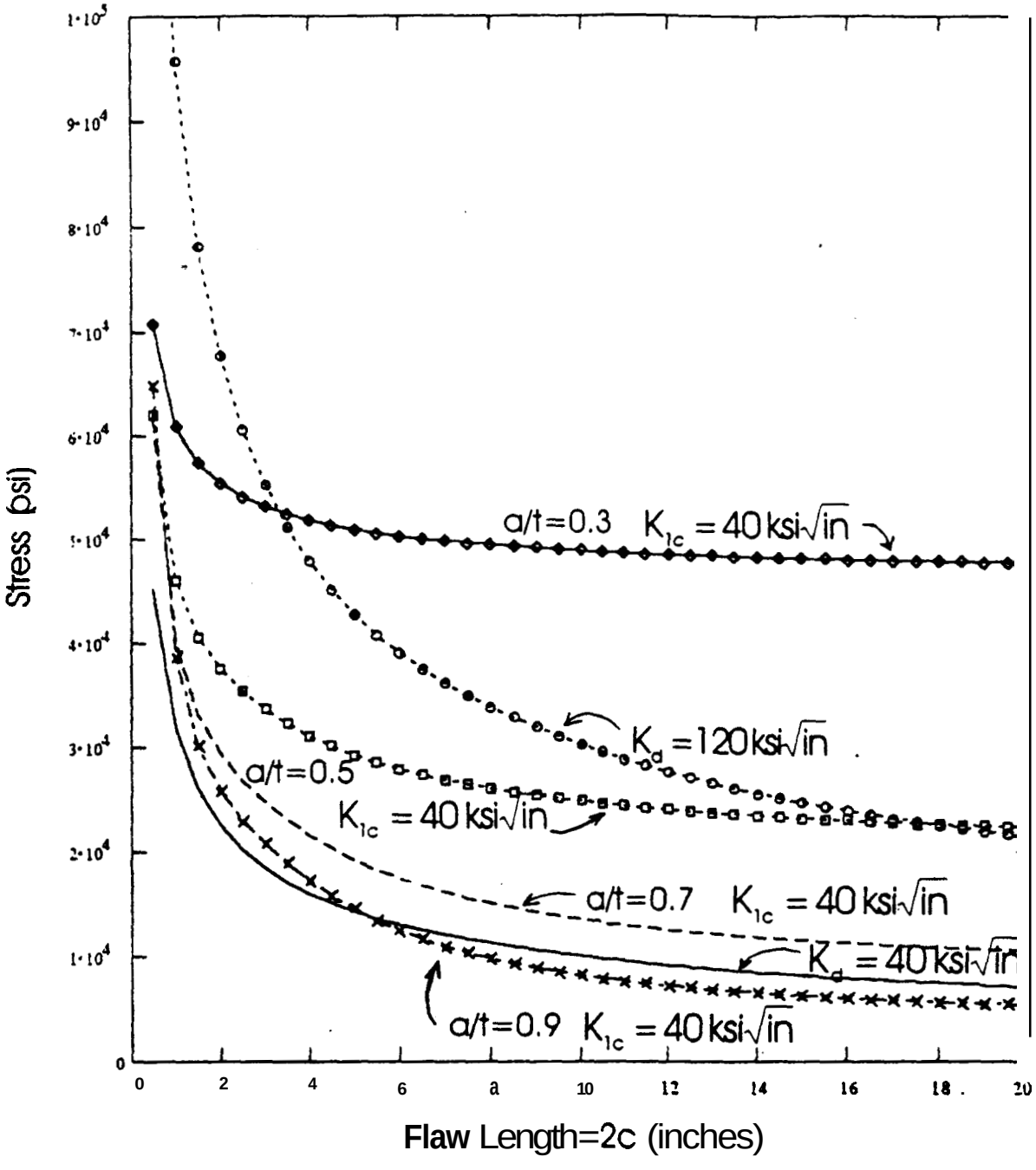


Figure 24 Stress required to give either pop-through of a part-through crack (curves labeled $K_{1c}$) or continued growth (curves labeled $K_d$). For a given stress and a/t value and initial flaw length 2c, if the stress required to give "crack pop-through) is larger than the stress required to cause the crack to continue to grow, then leak-with-rupture occurs. Note all curves are elevated as the value of critical stress intensity is increased, as *can* be seen by comparing the two curves for $K_d$=40 and 120 Ksi $(in)^{0.5}$. Kd values of 120 Ksi $(in)^{0.5}$ might be observed while $K_{1c}$ ~ 40 Ksi $(in)^{0.5}$ if the part through crack in plane strain and the through crack is in plane stress.

3.3.1 *Calculation of J-integral Driving Force for Crack Growth as a Function of Crack Length*

The total J as a function of axial crack length "2c" in a pressurized cylinder is calculated by summing the elastic component of J and the plastic component of J. The elastic component of J, $J_e$ is calculated using the relationships [15].

$$J_e = K_I^2 / E' \tag{18}$$

$$K_I = \sigma_h \sqrt{\pi c_{eff}} M \tag{19}$$

with $\sigma_h$ equal to the hoop stress and $2c_{eff}$ equal to the effective crack length.
The term following the familiar formula for stress intensity for a through-crack in a wide plate is the Folias correction factor, which takes into account the curvature of the pipe, with

$$M = (1 + 0.52\,\lambda + 1.29\lambda^2 - 0.074\lambda^3)^{1/2} \tag{20}$$

and $\lambda = \frac{c}{\sqrt{Rt}}$ with 2c = through-crack length, R = pipe radius and t= the pipe wall thickness.

Note the Folias correction term, M, is small for shorter cracks, which are little affected by pipe curvature, but increase as the crack grows in length.

According to Irwin [18], a crack with a plastic zone around the crack tip behaves like a slightly larger crack in a fully elastic material. This effective crack length, $c_{eff}$, which is used in Equation (14), is the actual crack length plus an equivalent additional crack length to account for the effects of crack tip plasticity. The plasticity correction is given by [19].

$$c_{eff} = \left[ c + \frac{1}{1 + (P/P_o)^2} \right] \cdot \left( \frac{1}{\beta \Pi} \right) \left( \frac{n-1}{n+1} \right) \left( \frac{K_I}{\sigma_{ys}} \right)^2 \tag{21}$$

In this relationship, the "n" value is determined from fitting a Ramberg-Osgood relationship [18] to tensile test results for **X52** [21] and X60 [22] steel, as seen in Figure **25.** $P/P_o$ is the ratio of the pipe pressure of interest to the pipe pressure required to give yielding: in this case, 0.4, 0.5, 0.6, and 0.72. Beta is **2** for plane stress and ***6*** for plane strain, with a value of **2** used here since a through-crack in a thin walled pipe would nominally be in plane stress. $\sigma_{ys}$ is the yield strength in a non-strain hardening material or the average flow stress in a strain hardening material.

It should be noted that the Folias correction factor was not applied to the stress intensity in the calculation of the effective crack length, Equation (21). When this was tried in some

preliminary calculations, corrections found for longer cracks were larger than the actual crack sizes themselves. When combined with the Folias correction applied in Equation (19). the use of the Folias correction factor in the calculation of the effective crack length appears to overcorrect for the effect of curvature. For this reason, it was only used in Equation (19). but not in the calculation of the effective crack length in Equation (21).

No relationship suitable for calculation of the plastic component of J for an axial through-crack in a cylinder (or pipe) was found in the literature. Eiber et al. [23] have suggested the calculation of J using the product of the crack tip opening displacement, made using the standard Dugdale calculation, times the hoop stress, modified by the Folias correction factor (M), or

$$J_p = \frac{8a\sigma_f^2}{\pi E} \ln\left[\sec\left(\frac{M_1 \pi \sigma}{2\sigma_f}\right)\right] \qquad (22)$$

$$\sigma_f = 0.43(\sigma_{ys} + \sigma_{uts})$$

with the curvature correction factor M given by

$$M = (1 + 1.2987\lambda^2 - 0.026905\lambda^4 + 5.3555 \times 10^{-4} \lambda^6]^{0.5} \qquad (23)$$

with $\lambda$ again equal to $c/\sqrt{Rt}$ . While the Folias correction factors of Equations (20) and (23) appear to be different, in fact they are in agreement to within 10% over the range of $1 < \lambda < 5$. The problem with the use of the relationship for J in Equation (19) is that for longer cracks and for pressures corresponding to higher hoop stresses, the product of hoop stress times Folias correction factor, $\sigma * M$ is larger than the flow stress, $\sigma_f$, making the Dugdale analysis untenable and the relationship impossible to evaluate [23].

In view of the above, a relationship to calculate the plastic component of J for a through-crack in a plate of finite width was used [18] with the width allowed to go to infinity, resulting in the following relationship:

$$J_p = \alpha' \epsilon \sigma' a h_1 \left(\frac{P}{P_o}\right)^{n+1} \qquad (24)$$

with E', **a,** and $\sigma'$ being fitting parameters for the Ramberg-Osgood function fitted to tensile data (see Figure 25). **A** value for h, was extrapolated from tabular data and assigned a value of $h_1 = 5.59$. No Folias correction factor was used in the calculation of the plastic component of J above. However, it should be noted that since the highest hoop stress considered in this study was only 72% of the yield strength, the plastic component of J **was** a small fraction of the total J. The total J was calculated from Equation (18) and Equation **(22)** as follows [20]:

# Stress-Strain Curves and Best Fit Results

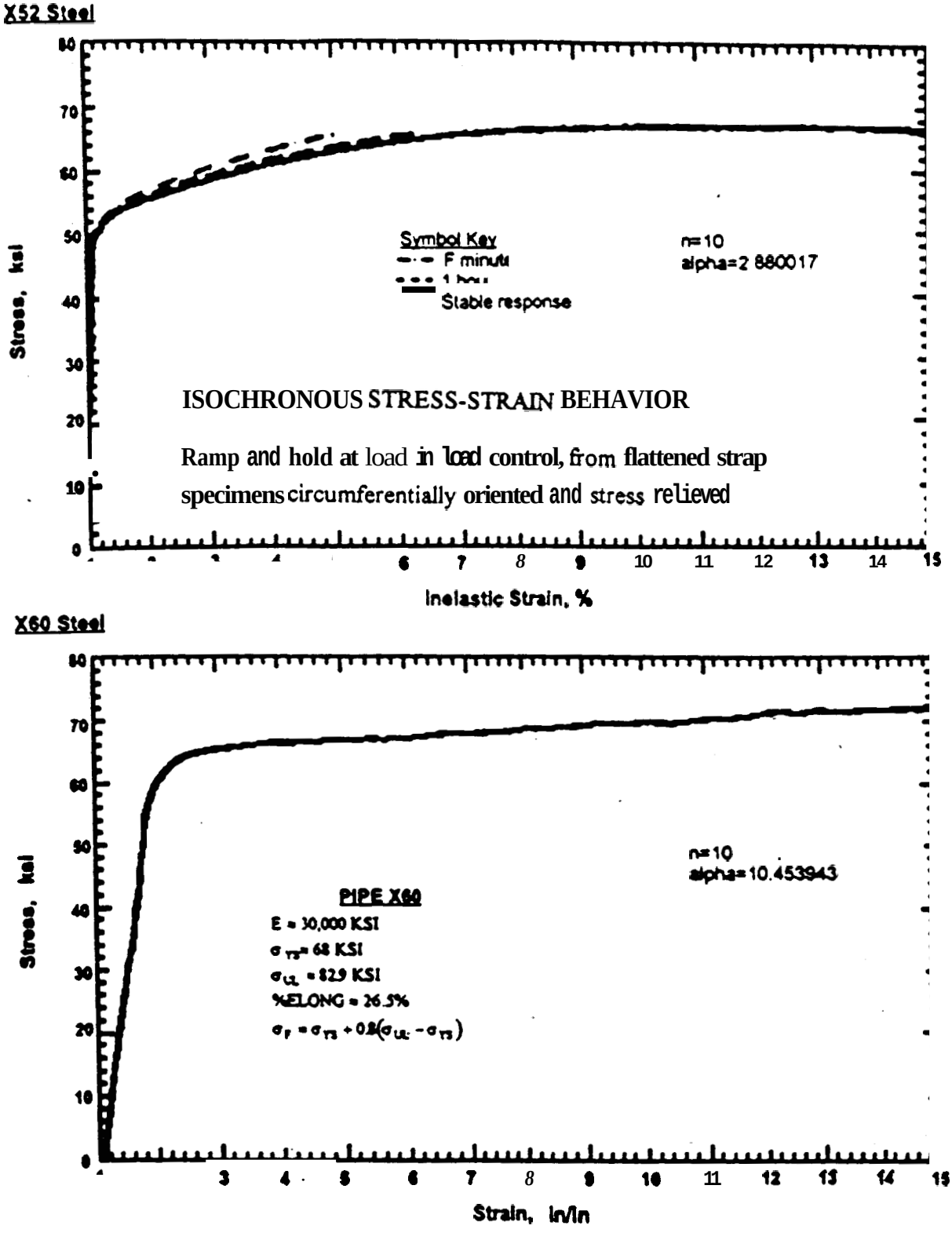


Figure 25 Ramberg-Osgood fit to tensile test data for X52 [21] and X60 [22] steel.

$$J_{total} = J_e + J_p \tag{25}$$

The results from this section are presented in tabular form in Appendix I. Representative results are seen in Figure 26.

### 3.3.2 *Determination of Critical Crack Length from Calculated J-c Curves and Measured J-R Curves*

**A** literature review was conducted to obtain measured values of the J-R, or J resistance curve, for X52 and X60 steel [23-25], with the results of the search presented in Figure 21. The J-R curve for X60 steel indicates a much higher toughness than the J-R curve for the X52 steel, which is consistent with the general observation that modem steels have higher toughnesses than earlier X52 steels. These curves for $J_R$ versus A c are presented graphically with the same scale as the J-c calculation in Figure *27.* The criteria for stable crack growth are

$$J, = J_R \tag{26}$$

$$\frac{dJ_1}{dc} < \frac{dJ_R}{dc} \tag{27}$$

while the criterion for unstable crack growth is

$$\frac{dJ_1}{dc} = \frac{dJ_R}{dc} \tag{28}$$

The criterion for unstable crack growth can be applied graphically by overlaying the $J_R$ vs. Ac curve on top of the J-c curve, sliding the $J_R$-$\Delta c$ curve along the x-axis until the curves intersect only at one tangent point. This point satisfies the criteria for unstable crack growth, or rupture. This procedure is illustrated for an X52 steel, 30-inch diameter, 0.375-inch wall thickness pipe at a hoop stress of 0.72 yield in Figure 28.

The value of $c_o$ which is indicated on Figure 28 is important for this analysis. Growth of an axial through-crack to a length of "$2c_o$" via fatigue or stress corrosion cracking sets the stage for unstable crack growth, resulting in rupture and catastrophic leakage. The values determined as described above for the flaw size, $2c_o$, which just precedes rupture for the various pipelines and steels included in this study are tabulated in Table 6. In the next section, these crack sizes will be used in combination with their associated pipe pressures to calculate the areas of opening that the crack produces in the pressurized pipes. These areas will in turn be used to calculate leak rates.

### 3.3.3 *Calculation of the Crack Opening Area for Axial Through-Cracks*

To determine the leakage rate for axial cracks, one must first determine the crack opening area through which the leakage will pass. Two references were found in the literature which calculated such areas. Paul [26] calculates the area using a relationship which considers only linear elastic behavior. His relation is:

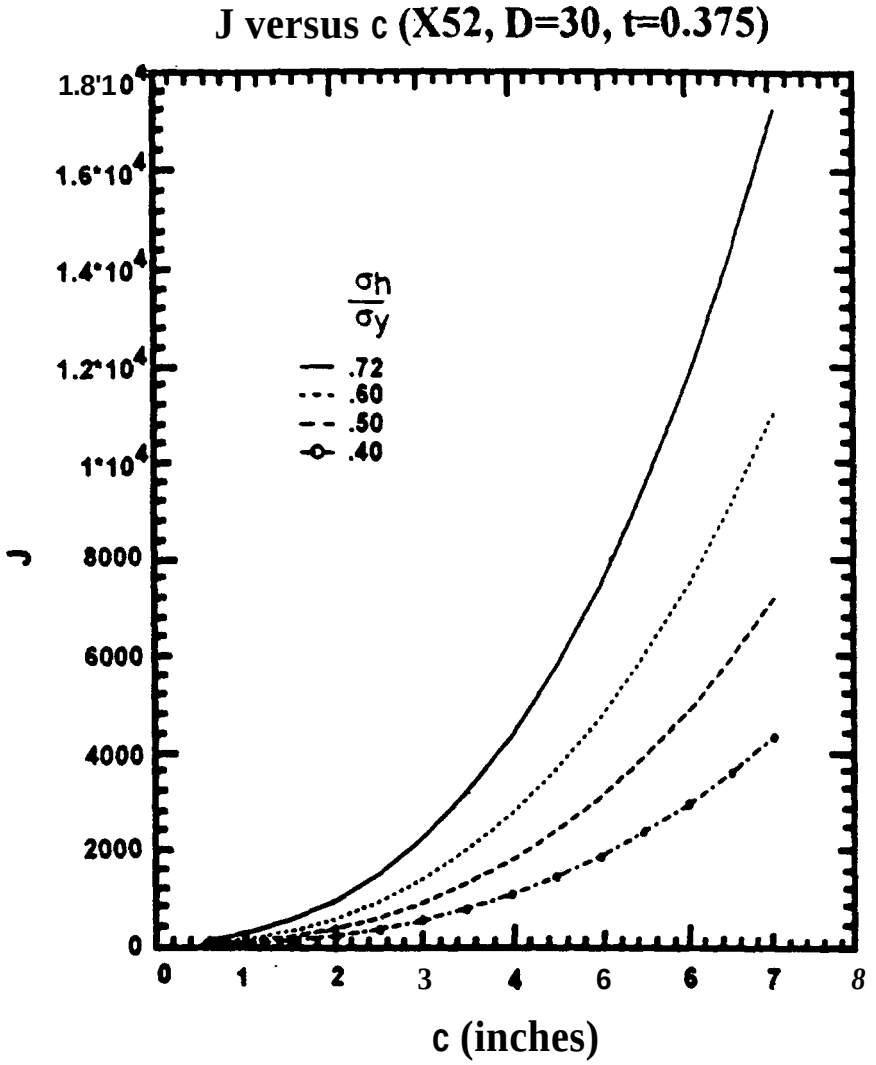


**Figure 26** Calculated J-c for X52 and X60 steel with a diameter of 30" and a wall thickness of 0.375 in.

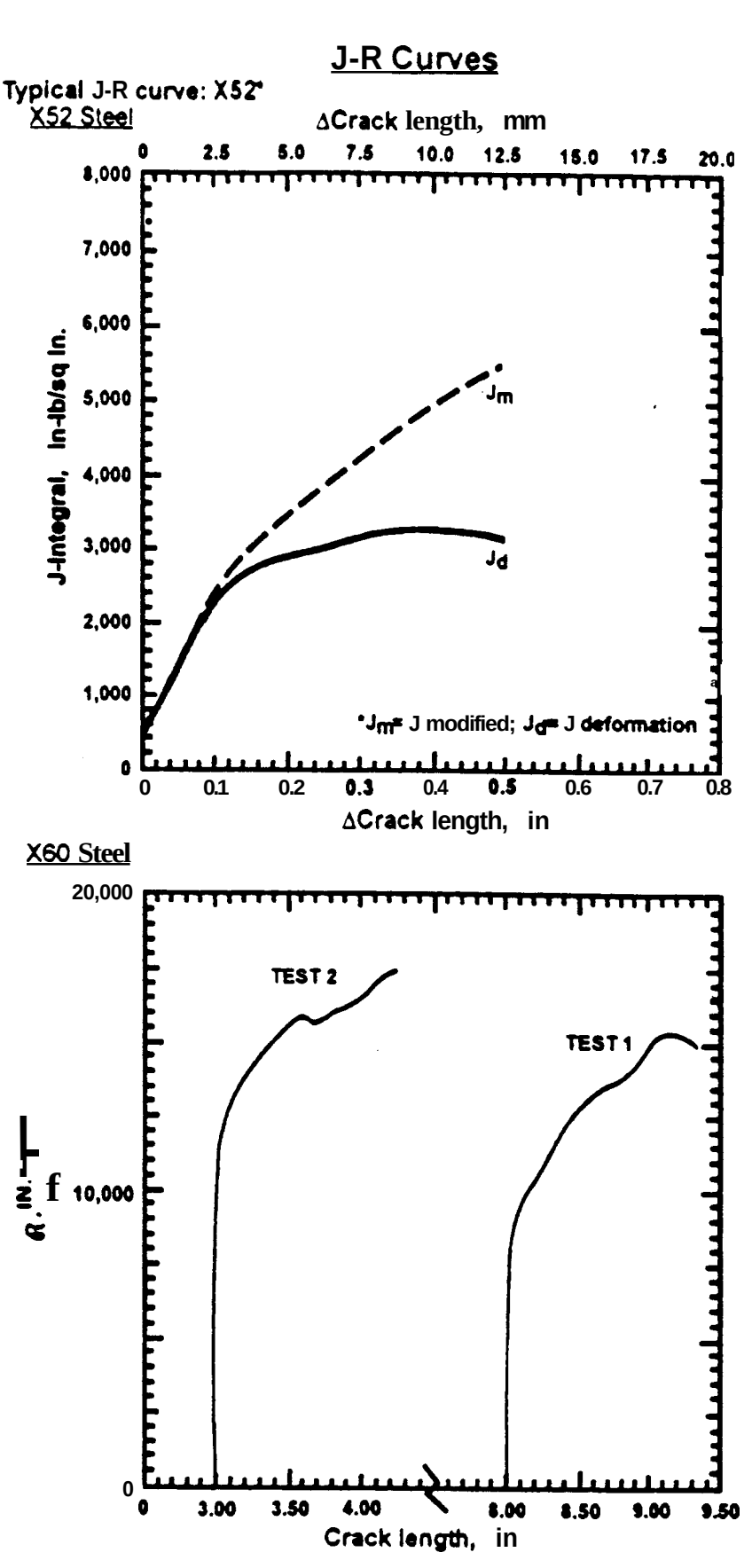


Figure 27 J-resistance (J-R) curves from measurements on X52 and X60 steel. The deformation $J_d$ was used in this work.

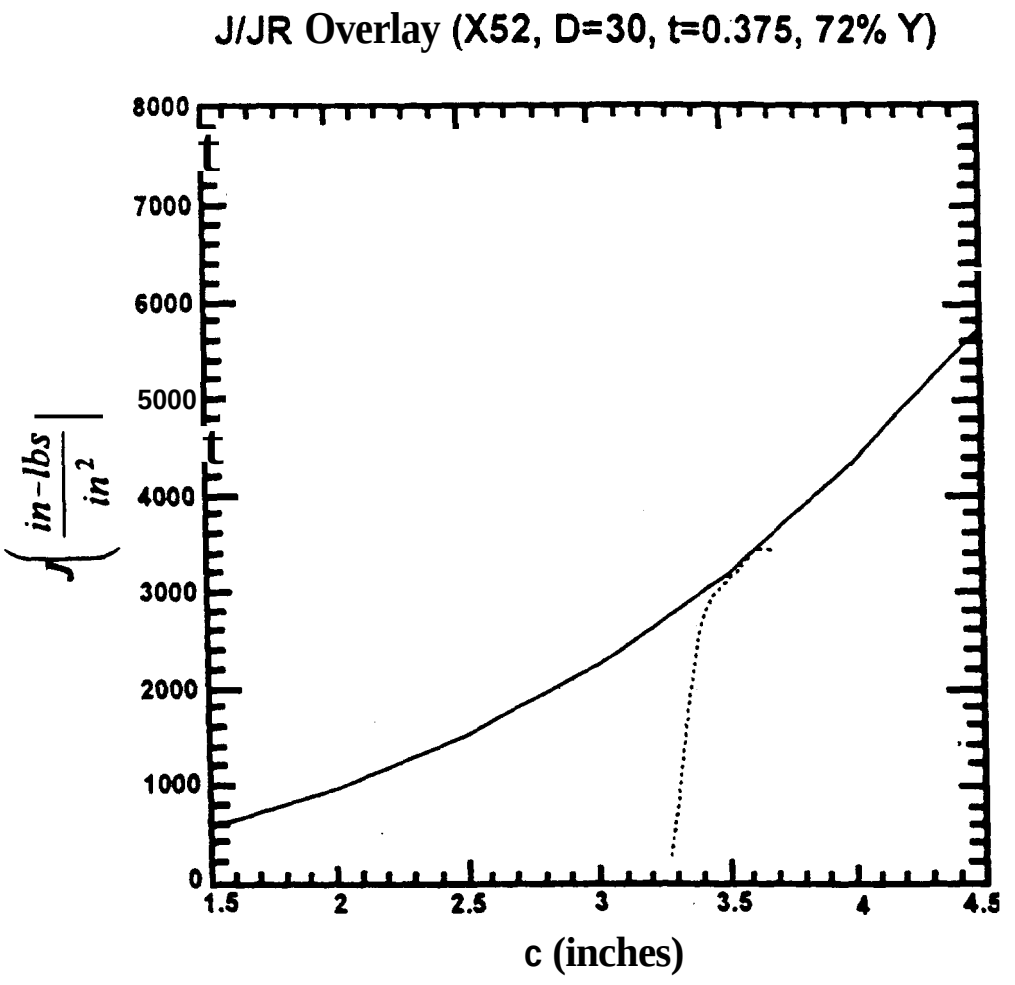


Figure 28 Determination of the critical crack length at which unstable crack growth and rupture occurs, using J-c calculated and J-delta-c as measured.

**Table 6** **Critical crack lengths, $2c_o$, at which an axial through-crack will give unstable crack growth and rupture for various pipe geometries and steels (X52 and X60)**

| Diameter (in) | 16 | 24 | 24 | 30 |
|---|---|---|---|---|
| Thickness (in) | 0.312 | 0.375 | 0.312 | 0.375 |
| | **X60 Critical Crack Length (in)** | | | |
| **% SMYS** | | | | |
| 0.72 | 8.45 | 10.15 | 9.58 | 10.96 |
| 0.6 | 10.33 | 12.48 | 11.73 | 13.49 |
| 0.5 | 12.42 | 14.90 | 14.15 | 16.15 |
| 0.4 | 15.40 | 18.54 | 17.49 | 20.03 |
| | **X52 Critical Crack Length (in)** | | | |
| 0.72 | 5.05 | 6.10 | 5.77 | 6.54 |
| 0.6 | 6.21 | 7.51 | 7.08 | 8.05 |
| 0.5 | 7.46 | 9.03 | 8.56 | 9.72 |
| 0.4 | 9.31 | 11.18 | 10.56 | 12.08 |

$$A_{elastic} = \frac{\sigma}{E}(2\pi Rt)G \tag{29}$$

$$G = \lambda^2 + 0.625\lambda^4 \qquad for \lambda < 1$$

$$G = 0.14 + 0.36\lambda^2 + 0.72\lambda^3 + 0.405\lambda^4 \quad for \lambda > 1$$

$$where \qquad \lambda = c/\sqrt{Rt}$$

Spiekhout [27] uses relationships based on an elastic-plastic analysis to evaluate the crack opening area. His relations are as follows

$$A_{elastic} = \frac{16\sqrt{2}\sigma c^2 \alpha}{3E} \tag{30}$$

$$where \quad \alpha = 1 + 0.1\lambda + 0.16\lambda^2$$

$$\lambda = \left[12(1-\upsilon^2)\frac{c^4}{R^2 t^2}\right]^{0.25}$$

$$\upsilon = Poisson's\ ratio$$

$$A_{elastic\text{-}plastic} = \alpha(1-x^3)\frac{A_{elastic}}{(1-x^2)^2}$$

$$where \quad x = 0.5\sqrt{2}\frac{\sigma}{1.1\alpha}$$

As a third possibility, one can simply integrate the elliptical crack shape of Paris and Sih [28] to obtain the following relationship

$$A_{elastic} = \frac{16}{3}\frac{K_1}{E}\frac{\sqrt{2}}{\pi}c^{1.5} \tag{31}$$

$$where \quad K_1 = \sigma\sqrt{\pi c}\, M$$

$$M\ is\ the\ Folias\ correction\ factor$$

One may compare these three analyses by considering a case which is typical of our interest. Assuming the following conditions,

R = 15" t = 0.375" 2c = 5.31" E = 30 x $10^6$ psi

$\sigma = .75\tau y$ $\sigma_y = 52{,}000$ psi $\upsilon = 0.3$

the respective area calculations give

$A_{\text{,,,,,,}} = 0.103$ (Paul)

$A_{elastic} = 0.129$ $A_{elastic\text{-}plastic} = 0.194$ (Spiekhout)

$A_{elastic} = 0.122$ (integration *of* elliptical crack shape)

where $A_{elastic}$ refers to results based on elastic analysis alone and $A_{elastic\text{-}plastic}$ refers to results based on elastic-plastic analysis. Since the elastic analyses were quite consistent and give reliable lower bound values for the crack opening area, it was decided to use the integration of the elliptical crack shape to get the areas of the various critical crack lengths at the four operating pressures of interest. These results are summarized in Table 7.

3.3.4 *Calculation* of *the Leakage Rate for Axial Through-Cracks*

Considerable literature for leakage rate calculations were reviewed, especially from the nuclear industry. It was decided to use an analysis by MPR [29], which utilizes the following relationship

$$\Delta P = \frac{w^2 v}{2A^2}\left(\frac{ft}{D_h} + K\right) \tag{32}$$

Where:

AP = Pressure Drop Across Crack
w = Mass Flow Rate (leakage rate)
v = Specific Volume of Fluid (1/p)
A = Crack Opening Area
t = Pipe Thickness
$D_h = 2A/2c_o$ Crack Hydraulic Diameter
K = Ki + Ke, Factor Describing Entrance and Exit Losses
f = Friction Factor (Function of Reynolds Number (Re) and Relative Roughness, see Reference [29]
$2c_o$ = Full Crack Length

Leakage rates were evaluated for the various pipes with internal pressures corresponding to $\sigma_h/\sigma_y = 0.4, 0.5, 0.6$ and **0.72.** Cracks of a critical size at different internal pressures investigated in this study for **X52** and X60 steel are summarized in Table 8.

3.3.5. *The Relationship Between Leakage Detection Limits and Limiting Pipe Pressures to Avoid Rupture.*

The preceding sections of this report have quantified the maximum leakage rate which one would have prior to rupture in a liquid pipeline with a through-crack. If one assumes a typical

**Table 7** The crack opcining area for various pipe geometries with axial through cracks that have reached these critical *sizes* for various internal pressures

| Diameter (in) | 16 | 24 | 24 | 30 |
|---|---|---|---|---|
| Thickness (in) | 0.312 | 0.375 | 0.312 | 0.375 |
| % SMYS | | | | |
| 0.72 | 0.62 | 0.82 | 0.75 | 0.93 |
| 0.60 | 0.90 | 1.21 | 1.09 | 1.38 |
| 0.50 | 1.25 | 1.65 | 1.54 | 1.89 |
| 0.40 | 1.81 | 2.42 | 2.21 | 2.75 |
| | | | | |
| 0.72 | 0.13 | 0.18 | 0.16 | 0.20 |
| 0.60 | 0.19 | 0.26 | 0.24 | 0.29 |
| 0.50 | 0.26 | 0.36 | 0.33 | 0.40 |
| 0.40 | 0.39 | 0.52 | 0.47 | 0.59 |

Table 8 Leakage rates for various pipes critical cracks of length $2c_o$ for four different internal pressures.

| Diameter (in) | 16 | 24 | 24 | 30 |
|---|---|---|---|---|
| Thickness (in) | 0.312 | 0.312 | 0.375 | 0.375 |
| | **X60 Leak Rate (gpm)** | | | |
| % *SMYS* | | | | |
| 0.72 | 810 | 803 | 955 | 973 |
| 0.60 | 1085 | 1079 | 1300 | 1325 |
| 0.50 | 1385 | 1388 | 1626 | 1669 |
| 0.40 | 1803 | 1792 | 2143 | 2179 |
| | **X52 Leak Rate (gpm)** | | | |
| % SMYS | | | | |
| 0.72 | 145 | 149 | 174 | 175 |
| 0.60 | 197 | 200 | 236 | 237 |
| 0.50 | 251 | 259 | 301 | 305 |
| 0.40 | 337 | 334 | 394 | 402 |

velocity for product in a pipeline to be **3** mph or 4.3 ft/sec, based on conversations with several industrial contacts, the leakage rates in Table 8 can be converted to percentages of through product transported. Then the rupture scenario can be described in terms of minimum leakage rates versus operating pressures or hoop stresses for pipelines made with X52 and X60 steels. The results of Table 8 with this normalization of the leakage rate are presented in Figure 29 and Table 9.

On the basis that a leak rate should be at least 8% of the throughput to be reliably detected, it is clear that the leakage rates associated with the critical crack sizes for X60 steel are sufficiently high that detection of leakage prior to rupture is highly likely. On the other hand, it is clear that the leakage rate for the X52 steel for the larger diameter to thickness ratios are in a range where detection is not certain. It may be possible to mitigate this situation if the time period between the first formation of the through-crack (by pop through) and the growth of the crack to a size that would give rupture is sufficiently long (which is possible, maybe even likely). Then one might still detect the leakage in time to avoid rupture by the accumulation of product around the through-crack location calling attention to the leak.

### 3.4 Conclusions and Recommendations for Hazardous Liquid Pipelines

**A** conventional leak-without-rupture analysis has been performed which clearly indicates that the pipeline operating pressure (or hoop stress), critical stress intensity, $K_{,,}$ , and the dynamic stress intensity, $K_d$ , are all important in determining whether the unstable growth of a crack through the wall continues as a running crack along the length of the pipeline. Safe operation of hazardous liquid pipelines, by which we mean leak-without-rupture, is possible at the current operating stress level of 0.72SMYS if and only if the pipeline steel meets certain requirements for quasi-static and dynamic fracture toughness, as measured by the critical stress intensities for these two conditions. Such a conclusion is a consistent with current understanding in industry [4], but defines the minimum required fracture toughness using critical stress intensities rather than Charpy V-notched tests or drop weight tear tests. For either approach, the operating temperature relative to the ductile to brittle transition temperature becomes a critical issue. Service leak-with-rupture scenarios in pipelines with a/t **- 0.7** and 2c–6 inches are readily explained with reasonable assumptions about the dyanmic and quasi-static stress intensities of the pipeline steels. Predictions of the probability of leak-before-rupture in pipelines as a function of hoop stress in general must wait the determination of a better data base of $K_{1c}$ and $K_{,,}$ as a function of temperature for **X52** and X60 steels.

In the analysis of leak-without-(eventual) break, it is clear that the use of tougher steels such as X60 can almost guarantee that leak-without-(eventual) rupture will occur with some certainty of leakage detection. On the other hand, lower toughness steels such as X52 with their small critical flaw sizes and attendant lower leakage rates prior to rupture pose a risk for rupture with the potential for loss of product and an associated environmental impact.

It should also be noted that the results in Table 8 and Figure 29 are lower bound values for leakage rates as they use crack areas which were calculated for elastic deformation only. However, the leakage rates calculated for the areas of the cracks may be overestimates in as much as the surface area to cross sectional area ratios for cracks with small surface opening may

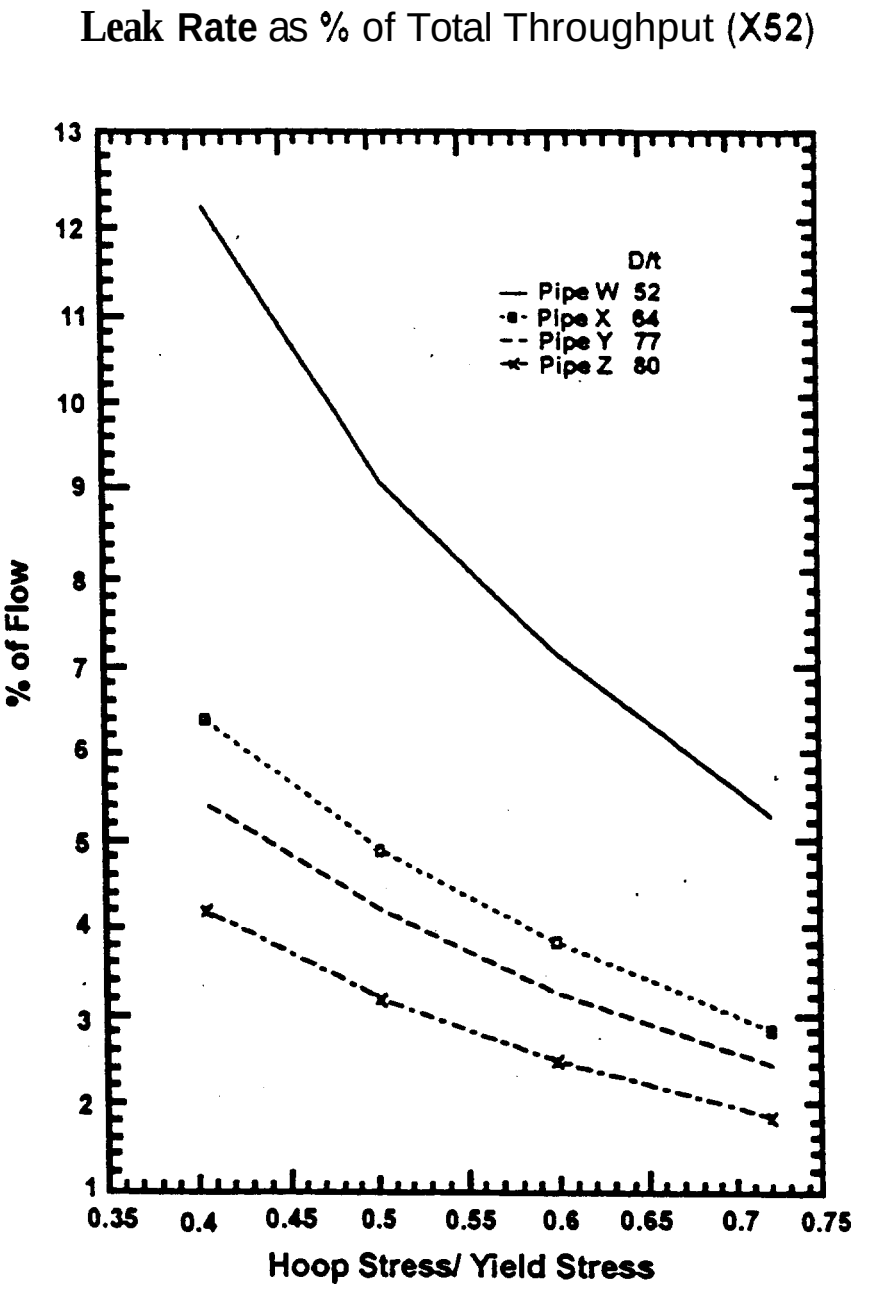


Figure 29a Leakage rate (% of flow) versus hoop stress/yield strength for various D/t ratios for X52 steel.

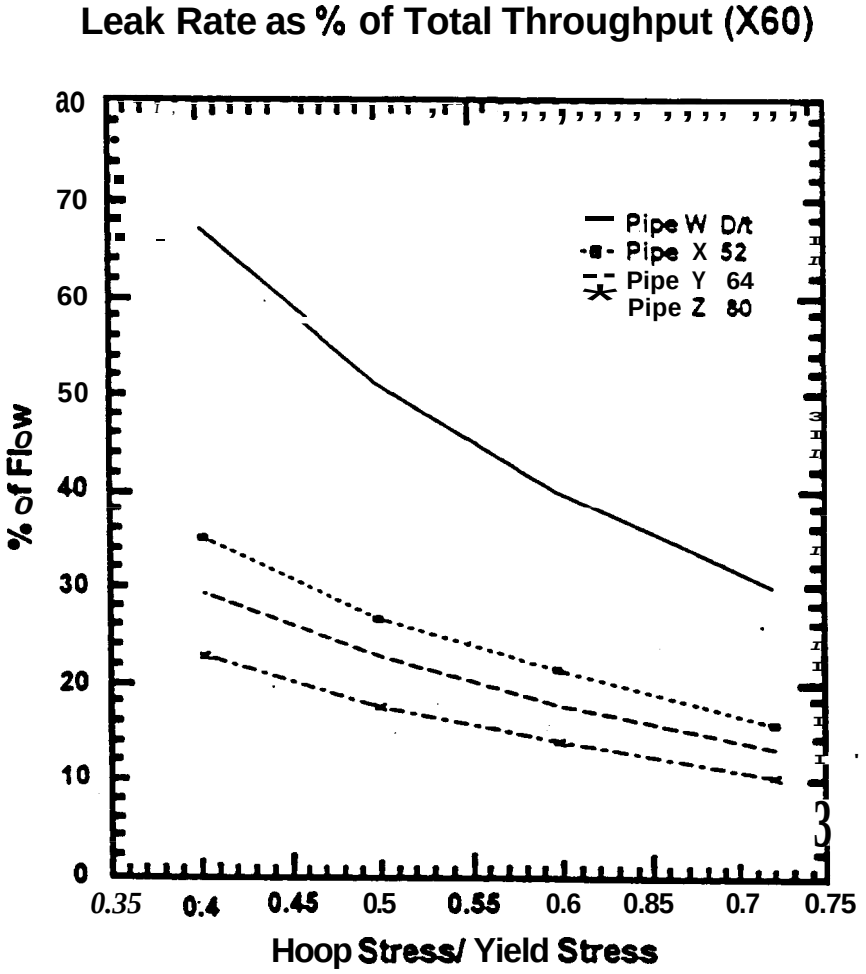


Figure 29b Leakage rate (% of flow) versus hoop stress/yield strength for various D/t ratios for X60 steel.

Table 9 Leakage rates (% of flow) as a function of $\sigma_f/\sigma_y$ ratio for pipes with through cracks of critical lengths.

| Diameter (in) | 16 | 24 | 24 | 30 |
|---|---|---|---|---|
| Thickness (in) | 0.312 | 0.375 | 0.312 | 0.375 |
| | | X60 – % of Flow | | |
| % SMYS | | | | |
| 0.72 | 29.4 | 15.4 | 12.9 | 10.0 |
| 0.60 | 39.3 | 21.0 | 17.4 | 13.7 |
| 0.50 | 50.2 | 26.2 | 22.4 | 17.2 |
| 0.40 | 65.4 | 34.5 | 28.9 | 22.5 |
| | | X52 – % of Flow | | |
| % SMYS | | | | |
| 0.72 | 5.3 | 2.8 | 2.4 | 1.8 |
| 0.60 | 7.1 | 3.8 | 3.2 | 2.4 |
| 0.50 | 9.1 | 4.9 | 4.2 | 3.1 |
| 0.40 | 12.2 | 6.4 | 5.4 | 4.1 |
| Flow Rate* (gal/min) | 2757 | 6204 | 6204 | 9694 |

* Assuming liquid is flowing through pipe at 3 miles/hour

be less than that indicated by Equation (32) due to the greater drag force exerted by the tight crack surfaces.

It is recommended that a subsequent study be undertaken to determine experimentally the critical stress intensities for quasi-static crack growth, $K_{1c}$, and dynamic crack growth, $K_d$, as a function of temperature for **X52** and **X60** steels using fatigue precracked, 2/3rds sized Charpy specimens. The transition temperature for dynamic and quasi-static fracture of standard V-notched specimens should also be determined for the same steels. The critical stress intensities could be used to predict the maximum operating pressures, to ensure leak-without-rupture.

## REFERENCES


[1] Anon., Evaluation of Accident Data and Federal Oversight of Petroleum Product Pipelines, National Transportation Safety Board, Washington, D.C. 20594, Report no. PB96-917002, NTSB/SIR-96/02, adopted January 23, 1996.

[2] Anon., Texas Eastern Transmission Corporation Natural Gas Pipeline Explosion and Fire at Edison, New Jersey, March 23, 1994, National Transportation Safety Board, Washington, D.C. 20594, Report no. PB95-916501, NTSB/PAR-95/01, adopted January 18, 1995.

[3] Anon., Pipeline Safety Regulations, U.S. Department of Transportation, Research and Special Projects Administration, Part 192.105, as revised October 1, 1994.

[4] Kiefner, John F., Maxey, W. A., Eiber, R.J. and Duffy, A.R., "Failure Stress Levels of Flows in Pressurized Cylinders," Progress in Flow Growth and Fracture Toughness, ASTM STP536, American Society for Testing and Materials, Philadelphia, pp. 461-481 (1973).

[5] Kanninen, M. F. and Popelar, C. H., Advanced Fracture Mechanics, Oxford University Press, New York, 1985.

[6] Freund, L. B., Dynamic Fracture Mechanics, Cambridge University Press, New York, 1990.

[7] Kanninen, M. F., Grant, T. **S.,** Demofonti, G., and Venzi, **S.,** "The Development and Validation of a Theoretical Ductile Fracture Model," Proceedings of the Eighth Symposium on Line Pipe Research, Paper no. 12, September 26-29, 1993, American Gas Association, Arlington, VA 22209, 1993.

[8] Priest, A.H. and Holmes, B., "The Characterization of Crack Arrest Toughness in Gas Transmission Pipelines in Terms of Shear Fracture Energy," British Steel Corporation, Commission of European Communities E.C.S.C. Sponsored Research Project Report, December, 1985.

[9] Wilkowski, G., Battelle Columbus Laboratories, Private communication, 1975.

[10] Maxey, W. **A.,** Kiefner, J. F., Eiber, R. J., and Duffy, A.R., "Experimental Investigation of Ductile Fractures in Piping," Proceedings of the 12th World Gas Conference, Nice, France, June, 1973.

[11] Kiefner, **J.F.,** Private communication *to* **M.F.** *Kanninen,* 1993.

[12] Eiber, R. J. and Bubenik, T. A., "Fracture Control Plan Methodology," 8th **A.G.A.** Symposium on Line Pipe Research, 1993, pp. 8-1.

[13] Chiovelli, D. V., Dorling, A. G., and Horsley, D. J., "NPS 36 Western Alberta Mainline Rupture at James River Interchange," 8th A.G.A. Symposium on Line Pipe Research, 1993, 26-1.

[14] McClure, G. M., Summary Report: Research on the Properties of Line Pipe, 1962, American Gas Association, 1962, pp. 1-133.

[15] Anderson, T. L., Fracture Mechanics: Fundamentals and Application, Ann Arbor: CRC Press, 1995, pp. 636.

[16] Irwin, G.R., "Plastic Zone Near a Crack and Fracture Toughness," Sagamore Research Conference Proceedings, Vol. **4,** 1961, pp. 100-105.

[17] Kumar, V., German, M. D., and Shih, C. F., "An Engineering Approach for Elastic-Plastic Fracture Analysis," EPRI Report NP-1931, Electric Power Research Institute, Palo Alto, CA, 1981.

[18] Anderson, T. L., Fracture Mechanics: Fundamentals and Applications, Ann Arbor: CRC Press, 1995, pp. 610-626.

[19] Leis, B. N., Goetz, D. P. and Scott, P. M., "Prediction of Inelastic Crack Growth in Ductile Line-Pipe Materials," 7th Symposium on Line Pipe Research, p. 16-11.

[20] Erdogan, F. and Ezzat, H., "Fracture of Pipelines and Cylinders Containing a Circumferential Crack," Welding Research Council Bulletin, Bulletin 288, October, 1983.

[21] Eiber, R. J., Maxey, W. A., Duffy, **A.** R., and Atterbury, T. J., "Investigation of the Initiation and Extent of Ductile Pipe Rupture," Battelle Columbus Laboratories Report BMI-1908, 1976.

[22] Leis, B. N. and Brust, F. W., "Model Predicts Crack Growth and Material Behavior,'' Oil and Gas Journal, Feb. 12, 1990, p. 47.

[23] Wilkowski, G. M., "Fracture Initiation Toughness Measurement Method," 6th Symposium on Line Pipe Research American Gas Association, Houston, TX, Oct. 29 - Nov. 1, 1979, p. G-17.

[24] Paul, R. S., "Axial Flaw Leak Rate," MPR Calculation No. 1064-TSL-2, April, 1993.

[25] Spiekhout, J., "Calculations Predict Leak-area in Gas Pipelines," ***Oil and Gas Journal,*** May 20, 1991, pp. 40-45.

[26] Paris, P. C. and Sih, G. C. M., ASTM STP 381, 1965, p. 30.

[27] MPR Calculation RNC 10-13-01, "Circflow Documentation (Version 2.0)," October **4,** 1990.